Desalination and Water Treatment
www.deswater.com
32 (2011) 226–233
August
1944-3994 / 1944-3986 © 2011 Desalination Publications. All rights reserved.
doi: 10.5004/dwt.2011.2704

In situ monitoring of membrane fouling in spiral-wound RO modules by UTDR with a sound intensity modeling

Genghong An[a], Jiebin Lin[a], Jianxin Li[a]*, Xiqi Jian[b]

[a]*State Key Laboratory of Hollow Fiber Membrane Materials and Processes, School of Materials Science and Engineering, Tianjin Polytechnic University, Tianjin 300160, P.R. China*
Tel. +86 (22) 2452 8072; Fax +86 (22) 2452 8055; email: jxli0288@yahoo.com.cn,jxli@tjpu.edu.cn
[b]*Department of Biomedical Engineering, Tianjin Medical University, Tianjin 300070, P.R. China*

Received 12 July 2010; Accepted in revised form 4 January 2011

ABSTRACT

The ultrasonic time-domain reflectometry (UTDR) technique with a new signal analysis protocol-sound intensity calculation and modeling was developed to detect the calcium-sulfate fouling in a commercial spiral-wound reverse osmosis (RO) membrane module. The fouling experiments were carried out with 2.0 g/L calcium sulfate solution. A 2.25 MHz focused transducer was used and mounted on the outside of the module housing. Results show that the ultrasound is capable to penetrate through the multiple layers of membrane. The systematic changes on the ultrasonic reflected signals with fouling time were observed by UTDR. The total sound intensity of the response signals obtained declined with the fouling time and reached a minimum at about 25 h of fouling, and then increased in the following time. The changes in the total sound intensity were correlated to the deposition and formation of the fouling. The entire acoustic spectra were divided into three sections according to the arrival time. The subsection sound intensity indicated that the fouling layers deposited on the membranes in regular order from inner to outer of the spiral-wound module. Gravimetric and scanning electron microscopy (SEM) analyses revealed the membranes near the pure water tube of the module suffered from much severely fouling. Overall, this study demonstrates that the UTDR with a suitable signal analysis protocol can provide valuable insight concerning fouling in a spiral-wound membrane module.

Keywords: Ultrasonic time-domain reflectometry (UTDR); Reverse osmosis; Spiral-wound membrane module; Membrane fouling; Sound intensity

1. Introduction

Membrane fouling is a critical problem in membrane-base liquid-separation processes, because it impairs the membrane performance such as increasing of trans-membrane pressure (TMP) and decline of flux, even the reduction of membrane life. The significant causes of membrane overfouling and abandoning in advance involve the deficiency of fouling early warning, the lack of on-line evaluation on scale inhibitor and cleaning agent as well as the membrane cleaning technology.

Indeed, the changes in flux and pressure are preferred to represent the fouling process in the invisible module. However, these methods have the inevitable limitation, which cannot recognize the exact fouling location and the details of fouling process on more complicated construction of spiral-wound reverse osmosis modules (SWROM). Other methods like that the SWROM is unwounded for

* Corresponding author.

Presented at the Third International Conference on Challenges in Environmental Science & Engineering, CESE-2010 26 September – 1 October 2010, The Sebel, Cairns, Queensland, Australia

fouling measurements can obtain full information of the fouling, but might result in damaging the module beyond retrieve. Therefore, the development of a non-invasive technique to study fouling mechanism so as to develop membrane cleaning technology is of great importance.

The methods used to try to nondestructively measure or monitor membrane fouling have included nuclear magnetic resonance spectroscopy (NMR) [1,2], CATSCAN [3], optical laser beam [4], optical methods [5,6], photography [7] and X-ray [8–11]. However, not all of the non-invasive methods can realize real-time observation to investigate the fouling in membrane separation processes. In the past ten years, substantial progress has been made in the application of a non-invasive ultrasonic time-domain reflectometry (UTDR) technique to membrane fouling and cleaning. Marial et al. [12,13] employed UTDR technique for the real-time characterization of calcium sulfate fouling and cleaning of flat-sheet RO membranes. The results showed a good correspondence between the declines in the ultrasonic signal amplitude and the development of a fouling layer. Li et al. [14] reported the interpretation of calcium sulfate deposition on RO membranes using UTDR and a simplified model. It showed that an increase in the relative amplitude of the fouling echo resulted from the build-up of the fouling layer. The simulated results were in good agreement with the actual observations obtained. Chong et al. [15] reported that two non-invasive techniques namely the sodium chloride tracer test and UTDR were employed to estimate concentration polarization (CP) level and monitor the growth of the silica fouling layer during the fouling process, respectively.

Further the UTDR technique was used to monitor the protein fouling on tubular ultrafiltration (UF) membranes with 13 mm inside diameter [16]. Recently, Xu et al. [17] developed the extension of UTDR for the real-time measurement of particle deposition in a single hollow fiber membrane. The systematic changes of acoustic responses from the inside surfaces of hollow fiber in the time- and amplitude-domain with the operating time were observed during the fouling experiments. Especially Zhang et al. [18] described the extension of UTDR for the measurement of fouling and cleaning in commercial spiral-wound membrane modules. They introduced two shift factors based upon changes in the signal amplitude and arrival time to analyze the incomprehensible acoustic response respectively. Upon further investigation, Chai et al. [19] employed UTDR associated with gravimetric and scanning electron microscopy (SEM) analyses to study on the fouling in spiral-wound membrane modules and found the changes of signal amplitude seem more sensitive than that of flux. Four particular peaks which emanated from specific surfaces were selected from the waveform response as the observed signals to track their changes with the fouling process in their studies. Moreover, Hou et al. [20] described UTDR as a non-invasive real time technique for in-situ monitoring of the early-stage $CaSO_4$ and microbial synergistic fouling on nanofiltration (NF) membranes. The results showed that bacteria could accelerate deposition of inorganic fouling on NF membrane.

This review demonstrates that there is a need to apply UTDR for studying for fouling in geometries other than the flat sheet. Although the progress on monitoring spiral-wound module with UTDR has been made, the above shift factors and particular signals were not quantitatively associated with information on the specifics of the fouling process such as the location, coverage, structure or distribution of the deposits. A major challenge is to explore a more detailed and suitable analysis of the ultrasonic response signals in order to ascertain the nature of the fouling process due to the multiple curved surfaces of the spiral-wound membranes leading to complex reflection signals and increased signal attenuation [21–24]. Hence, the present study aims to develop UTDR with a signal analysis protocol i.e. sound intensity calculation and modeling to monitor the fouling in a spiral-wound membrane module so as to reveal the influence of spiral-wound module design and hydrodynamics on the particular structure and distribution of fouling deposits. Gravimetric and SEM analyses were used to corroborate the ultrasonic results.

2. Methods

2.1. Spiral-wound RO and UTDR measurement systems

The set up of the spiral-wound RO and ultrasonic measurement systems is shown in Fig. 1. The assembly consisted of three 100 L feed tanks for storage and supply of the feed solution and pure water, a cooling system for the feed tanks, a feed pump and a high-pressure pump for pressurization of the feed solution. Two conductivity meters (C_1 and C_2) were installed to measure the concentration of the feed and permeate. Permeate and retentate streams measured with flow meters were circulated back to the feed tank. A 4-inch commercial spiral-wound RO module with 452.5 mm length and 91.25 mm diameter and stainless steel module housing with 105.5 mm outside diameter and 2 mm thickness were used in this study. Thus, the distance between the inner module housing surface and module wrapping is 5.1 mm. The UTDR measurement system comprised a 2.25 MHz focused ultrasonic transducer mounted on the outside of the module housing at one third of the length near the down stream, a pulser/receiver, a digital oscilloscope and a computer.

2.2. Experimental procedure

The experiments were conducted with two phases: water equilibration phase (15 h) to achieve steady states of membrane module performance and UTDR signals, and fouling phase (45 h) with 2.0 g/L calcium sulfate solution based on the saturation concentration of calcium sulfate of 2.4 g/L at 25°C. All experiments were carried

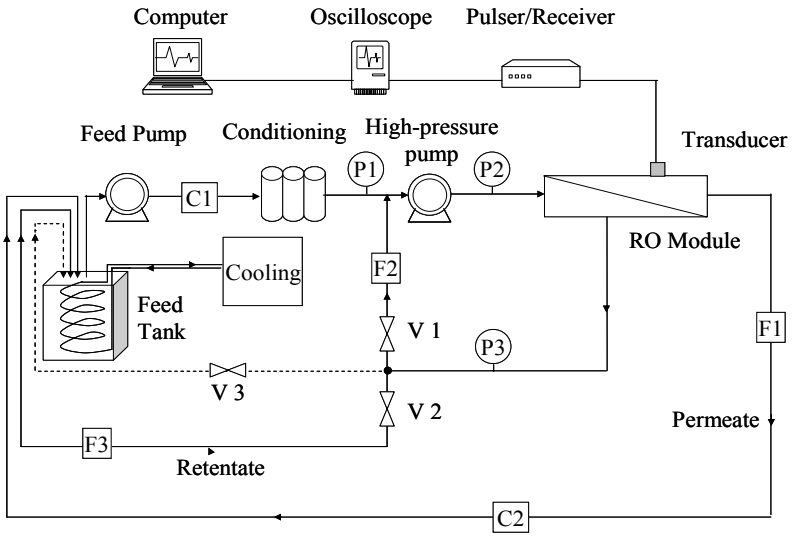

Fig. 1. Schematic diagram of the spiral-wound RO and ultrasonic measurement systems.

out at the same operation pressure of 1 MPa, temperature of 25±1°C, and retentate flow rate of 60 L/h. During the experiment, the data of temperature, conductivity, flux and corresponding ultrasonic echo signals were collected at regular intervals. After each experiment, the fouled module was firstly removed from the housing and dried at room temperature for two weeks for the gravimetric and SEM analysis. The fouled envelope layers under the transducer were counted and marked from outmost to innermost (closest to the pure water tube) with 1st to 27th before the module was unrolled. Then the marked envelope layers were carefully cut into a narrow rectangle with 20 mm width along the axial direction which was marked A through G along the orientation of feed flow at intervals of 55 mm. The membranes in the first three marked layers were partly or wholly sealed by the glue. The last two subsections were fixed to pure water tube with the adhesive and hard to ensure that the fouling deposit was not lost. Therefore, only the marked envelope layers from the 4th to the 25th subsections were further cut into the same area with 55 mm length and 20 mm width. The fouled membrane samples along the axial and radial orientation of the SWROM were then collected for weight measurements and morphological analysis by SEM.

3. Results and discussion

3.1. Fouling experiments

The pure water flux remained essentially constant at 50 L/m^2·h on average during the water equilibration phase. The steady state was attained and the feed was switched to calcium sulfate solution to initiate the fouling experiment. Permeate flux and feed conductivity vs. fouling time is summarized in Fig. 2. As shown in Fig. 2, The permeate flux declined rapidly at the commencement of fouling phase and reached to about 50% of its initial value after 10 h of fouling operation, and then gradually dropped to 10% of its initial value (18 L/m2·h) at the end of the fouling experiment. The permeate flux decline primarily results from concentration polarization and calcium sulfate fouling. The saturation concentration of calcium sulfate is 2.4 g/L at 25°C. The calcium sulfate precipitates from the high feed solution (2.0 g/L) onto the membrane surface when super-saturation occurs due to concentration polarization. It can also be seen from Fig. 2 that the conductivity of feed solution rapidly decreased from 1987 μs/cm to 1224 μs/cm at the initial 10 h of fouling and then kept relatively stable. This implies that a part of calcium sulfate in feed solution deposited on the membranes in SWRO module. The rejection had a slight drop from 97% to 96% through the fouling phase. These observations indicated that the whole membrane module suffered from the severe fouling.

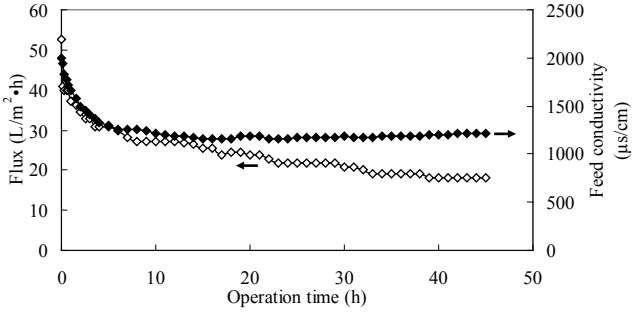

Fig. 2. Permeate flux and feed conductivity vs. fouling time.

3.2. Ultrasonic measurements and modeling protocols

Ultrasonic measurements are based upon the propagation of mechanical waves. The velocity of the waves is dictated by the medium through which they travel. When an ultrasonic wave encounters an interface between two media, the energy partition is controlled by the ultrasonic impedance contrast of them. According to the UTDR measurement principles, the arrival time of echo signals are related to the distance between the reflecting interfaces and the transducer [19].

In the most of the previous studies, UTDR was used to investigate fouling on simple flat-sheet [12], single tubular [16], and single hollow fiber [17] membranes. Their corresponding acoustic waveforms contain only several peaks reflected from a few interfaces and are easily analyzed. However, the signal analysis is much more complicated when the UTDR is applied to a spiral-wound RO membrane module due to the multiple reflections from the outer and inner surfaces of the viscous coupling agent, the module housing, element wrapping material, concentric membrane layers, membrane support layers and channel spacer layers as shown in Fig. 3a. A typical and complicated UTDR waveform corresponding to the spiral-wound module plotted as the signal amplitude in volts (V) vs. the arrival time in seconds (s) inside the spiral-wound RO module is shown in Fig. 3b. It is found from Fig. 3b that significant signal attenuation with the arrival time can be observed as a result of the energy partition through these layers. At the same time, the peaks in the acoustic waveforms represent very complex superposed reflections from the many close-packed interfaces [18]. The reflections also include the multiple reflections from the housing. The key point for the UTDR measurements is to identify the reflections or reflection region from the membrane layers. In order to ascertain the approximate arrival time corresponding to the reflected signal of each main interface, the arrival time for the peak generated from the inner surface of module housing (stainless steel) was calculated to be 3.55 μs according to the UTDR measurement principles [14]. It is noted that the sound velocity in stainless steel is 5000 m/s and the arrival time from the focused transducer surface to the outside surface of the module housing is 1.75 μs. To prove this result, an experimental by ultrasonic measurements was carried out with the empty and water-filled module housing. Thus the differential signal was obtained by subtracting the acoustic spectra of the water-filled module housing from that of the empty module housing as shown in Fig. 4. The arrival time for the peak corresponding to the inner surface of module housing is 3.5 as. It is close to the calculated result above.

Based upon the above observations and the assumption that the ultrasonic velocity in water and waterish module is 1500 m/s and 1800 m/s respectively, the reasonable arrival time of reflection signals corresponding to the region from module wrapping to pure water tube obtained is from 10 μs to 60 μs (Fig. 3b). In consequence, the following signal analysis focuses on the reflection

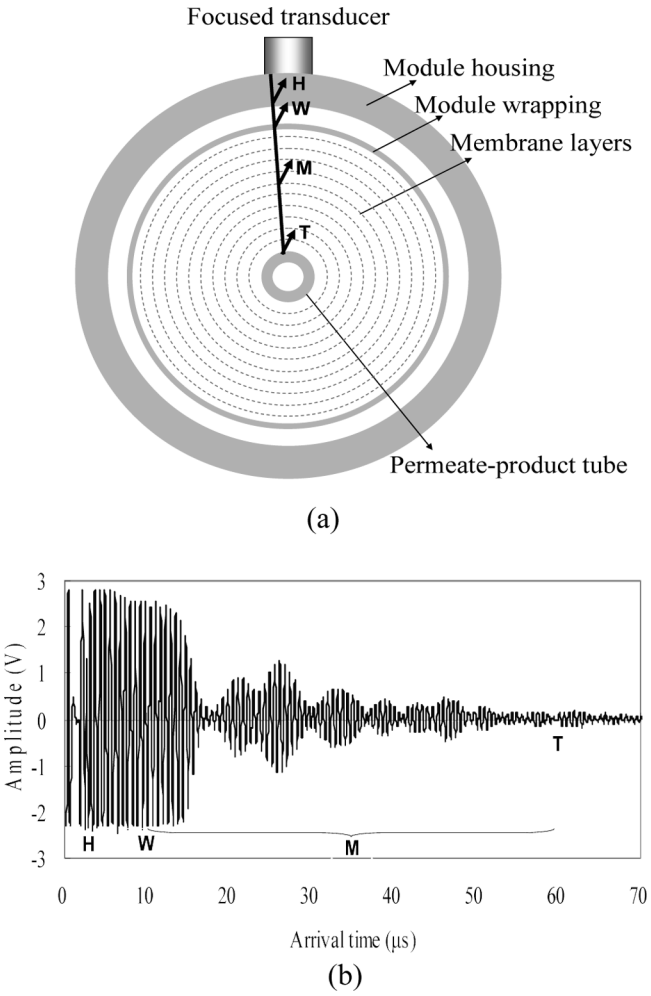

Fig. 3. Cross-sectional view of the spiral-wound membrane module (a) and corresponding to the ultrasonic spectra (b).

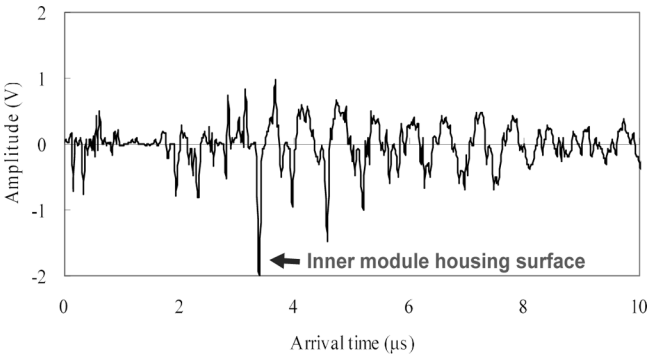

Fig. 4. Differential signal obtained from the inner surface of module housing.

signals within this arrival time region as the changes of the waveform in this portion of spectrum contain the information from the layers of the membrane element.

The ultrasonic echo signal spectra after 5 h, 25 h and 45 h of fouling operation obtained are shown in Fig. 5. Similar to the observation from Fig. 3, Fig. 5 shows each ultrasonic signal spectra attenuation in amplitude-domain with the arrival time during the fouling phase. By contrast with the pure water filtration, the systematic changes on the signals corresponding to the membrane layers can be observed throughout the fouling phase in Fig. 5. In total, the amplitudes of peaks reduced at the beginning of the fouling experiment (Fig. 5a) and partly resumed in the following operation (Fig. 5b). However, individual peak which represents complex superposed reflection from the close-packed interfaces shows different variation exactly and the nature of fouling processes. In order to overcome the challenges in the complicated signal analyses and promote the utilization of UTDR for practical application, a new signal analysis protocol namely sound intensity calculation and modeling was developed and shown in Fig. 6.

As shown in Fig. 6, based upon the original ultrasonic signals measured at each fouling time, the corresponding modeling spectrum of ideal sound wave is obtained by the Mathematica software (Wolfram Research Inc.). The sound intensity at each fouling time could be calculated according to the relative parameters such as sound pressure, density, sound velocity etc. obtained from the simulated spectra. Herein, the sound intensity is defined as the amount of energy flowing per unit area per unit time and proportional to the square of the acoustic amplitude. Finally, the change of sound intensity with fouling time is obtained. The sound intensity calculation and modeling is illustrated in detail as follows.

With the presented protocol, each entire acoustic spectrum of the reflection signals was divided into three subsections according to the arrival time, i.e.: L1 from 10.9 to 17.2 μs, L2 from 18.4 to 30.2 μs, and L3 from 30.6 to 41.5 μs as shown in Fig. 5. The effects of 20, 38 and 38 semi-sinusoidal waves were then simulated respectively for each subsection above using Mathematica software (Wolfram Research Inc.). To simulate the effect of semi-sinusoidal, three factors were required for the sine function equation expressed as Eq. (1) [25]:

$$P_i(t) = A_i \sin\left[\frac{2\pi}{T_a}(t - t_0)\right] \quad (1)$$

where T_a is the average period of each subsection, A_i, the amplitude of peaks, and t_0, the phase angle determined by the arrival time of peaks.

While the subsection of a spectrum is given, these factors can be confirmed. Fig. 7 shows a representative simulated spectrum of L1 in comparison with original spectrum plotted by Mathematica software.

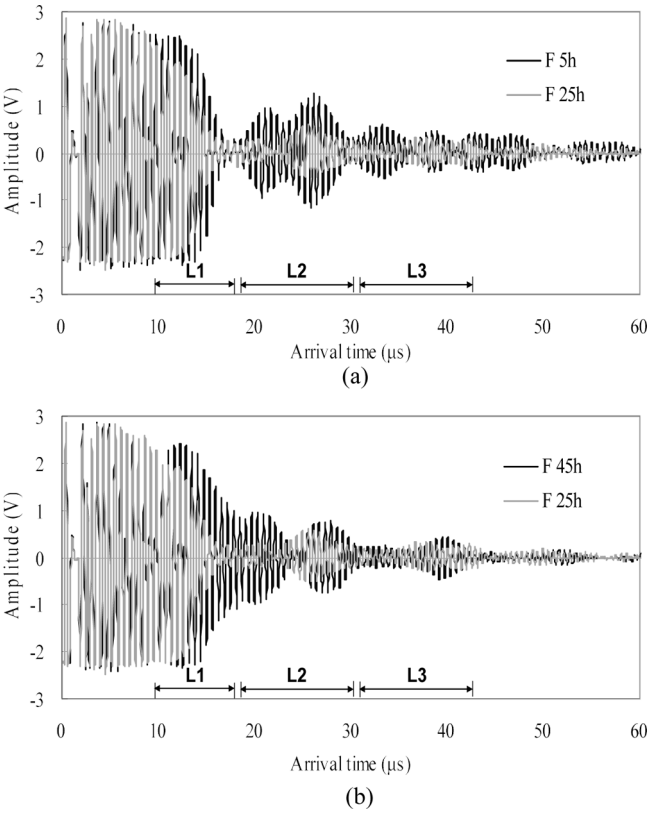

Fig. 5. Ultrasonic signal spectra obtained in the fouling phase.

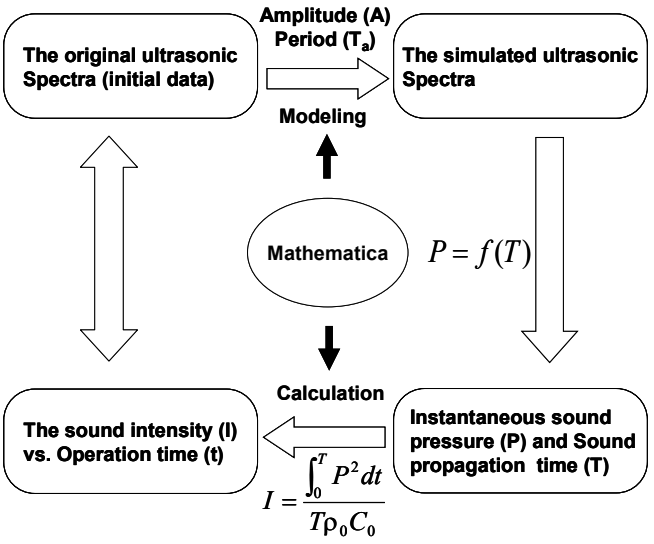

Fig. 6. A new signal analysis protocol - sound intensity calculation and modeling.

The sound intensity I is determined from the following equation [25]:

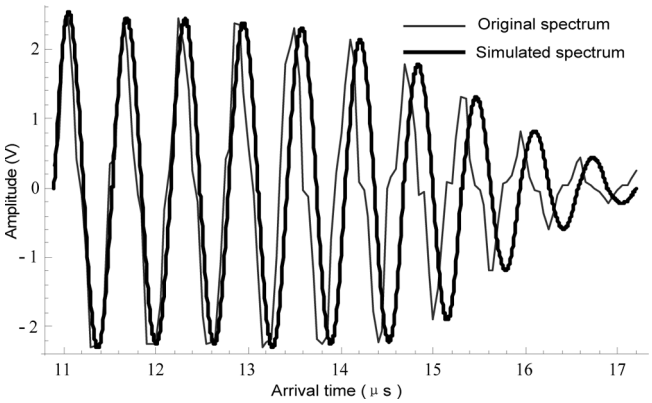

Fig. 7. Representative simulated spectrum in comparison with original spectrum.

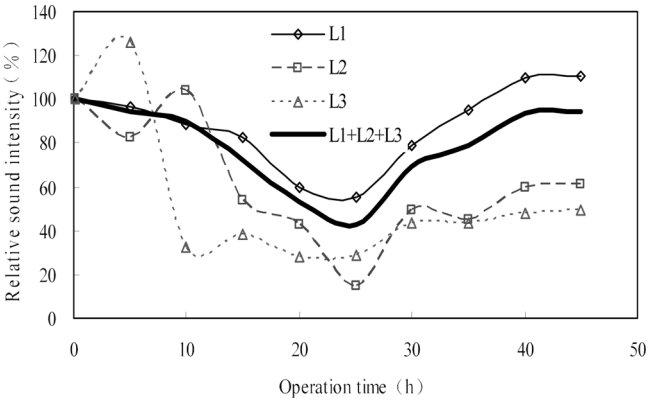

Fig. 8. Changes of each subsection sound intensity in the fouling phase.

$$I = \frac{P_e^2}{\rho_0 C_0} \tag{2}$$

where P_e is the sound pressure in the interval of T, P_e can be given by

$$P_e = \sqrt{\frac{1}{T}\int_0^T P^2 dt} \tag{3}$$

Combining Eqs. (2) and (3), yields

$$I = \frac{\int_0^T P^2 dt}{T\rho_0 C_0} \tag{4}$$

where ρ_0 is the medium density and C_0 is the ultrasound velocity in the medium. Therefore, the subsection sound intensity (W/m^2) can be obtained by Eqs. (1)–(4), and total sound intensity is the sum of sound intensities of the three subsections.

The reference spectrum was obtained, corresponding to "zero" fouling operation time at which fouling has not occurred. Changes in the subsection and total sound intensities as a function of operation time are determined based upon their shifts from the sound intensity of the reference spectrum. Thus the relative subsection and total sound intensities were calculated and plotted in Fig. 8. As shown in Fig. 8, the total sound intensity of the response signals slightly decreased to 90% after 10 h of fouling time and reached a minimum of 40% after 25 h of fouling, and then increased in the following fouling time.

The change of total sound intensity is associated with the concentration polarization and $CaSO_4$ fouling. On the membrane surface, when the increasing concentration which is induced by concentration polarization and increases gradually along the flow channel exceeds the salt saturation level, the precipitation and fouling occurs [26]. The growing precipitate under the transducer interfered with the echo signal from the module by absorption and scattering, and the sound intensity abated gradually. However, once a fouling layer formed, an intensive reflected wave occurred from the water/fouling interface due to the calcium-sulfate density of 2.61 g/cm^3 which ultrasonic impedance is higher than that of polymeric membrane materials. Thus the sound intensity would partly resume with the formation of a reasonably thick and even fouling. The change of sound intensity obtained is consistent with the change of amplitude as a result of membrane fouling in a flat-sheet module with controlled hydrodynamics reported by Mairal et al. [13].

In addition, it can also be seen in Fig. 8 that the change of individual subsection intensity with the fouling time is similar to that of the total intensity obtained. Furthermore, an interesting phenomenon is that the subsection intensity descended orderly from L3 to L1 at the initial fouling time. This suggests that the fouling deposited on the membranes in regular order from inner to outer of the spiral-wound module. These observations will be further confirmed by the following gravimetric and SEM analyses (as shown in Figs. 9 and 10).

3.3. Gravimetric and SEM analyses

The membrane module after the fouling operation was taken for the gravimetric and SEM analyses to study the fouling formed on the membrane surface so as to confirm the ultrasonic measurements. The fouled membrane samples were cut as mentioned above and marked A through G along the feed flow direction. The specimens marked F were related to the area detected by the mounted transducer during the experiment.

SEM micrographs of fouled membrane samples obtained from the membrane specimens on the location marked F along the permeate flow direction of the spiral-wound RO module are illustrated in Fig. 9. Obviously, the fouling coverage increased gradually along the permeate flow direction of the spiral-wound RO module towards the center of the module, which was consistent

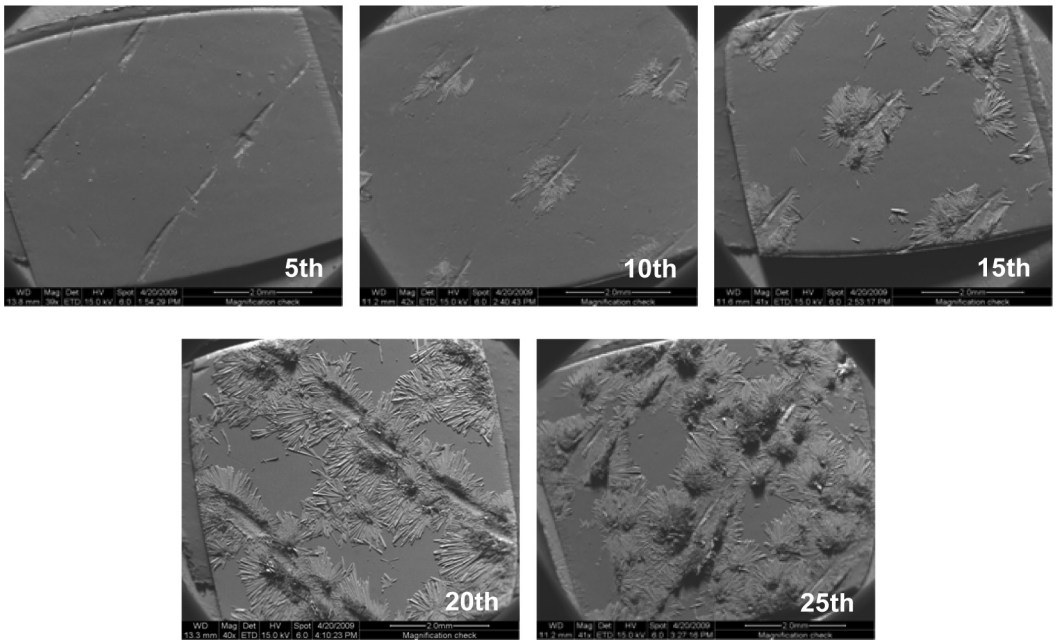

Fig. 9. SEM micrographs of (a) fouled membrane samples obtained from the envelope membrane layers (5th, 10th, 15th, 20th and 25th) on the location marked F along the radial orientation of the spiral-wound RO module.

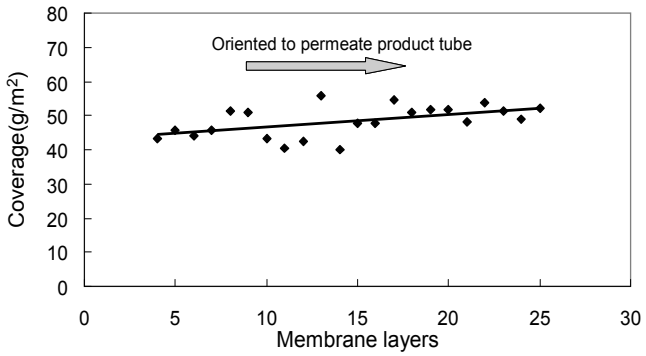

Fig. 10. Fouling coverage along the radial orientation of the spiral-wound RO membrane.

with the results obtained by the gravimetric analysis (Fig. 10). The $CaSO_4$ coverage gradually increased from 42.25 g/m^2 at 5th envelope membrane layer to 52.21 g/m^2 at 25th layer. Those observations were in agreement with the results obtained by Mairal et al. [13] and Chai et al. [19]. A possible explanation is that the small circumferential pressure drop associated with the spiraling permeate flow induces the feed flow to spiral as well [19]. If so, the calcium-sulfate concentration in the feed would increase towards the center of the module and thereby cause more fouling. It is quite likely that the increase in feed-channel spacing will be less than near the inner membrane envelope layers owing to the restraining influence of the rigid permeate-product tube. On that basis, the shear will be less within the inner relative to outer feed-channels and thereby result in more fouling near the center of the module. Consequently, these SEM results and the gravimetric measurements well corroborated with the ultrasonic measurements obtained. It suggests that the fouling deposits increase in the direction of the permeate flow.

4. Conclusions

An ultrasonic time-domain reflectometry with sound intensity modeling has been shown to be a powerful measure for non-invasive observation of sulfate calcium fouling in a spiral-wound reverse osmosis module. The systematic changes in the entire acoustic spectrum with the operation time during the fouling experiment indicate that the ultrasound generated by the focused transducer is able to penetrate through the module housing and propagate into the multiple layers of membrane as well as monitor fouling in real time. With the new signal analysis protocol - the sound intensity calculation and modeling, UTDR can quantify the changes of acoustic responses. Results show that the sound intensity of the reflection abated when the fouling occurred, and partly resumed when a reasonably thick fouling formed. Further, the subsection intensities show that the fouling deposited on the membranes in regular order from inner to outer of the spiral-wound module. The membranes close to the pure water tube suffered from relatively serious fouling. Overall, gravimetric and SEM analyses corroborate the ultrasonic measurements.

Acknoweledgements

The authors gratefully acknowledge the National Natural Science Foundation of China (Nos. 20676100 and 20876115) and the SA/CHINA Agreement on Cooperation on Science and Technology (No. 2010DF51090) for the financial support. The authors also appreciate Professor Ron Sanderson from University of Stellenbosch, South Africa for his helpful discussion.

References

[1] E.J. La Heij, P.J.A.M. Kerkhof Kopinga and L. Pel, Determining porosity profiles during filtration and expression of sewage sludge by NMR imaging, AIChE J., 42 (1996) 953.
[2] D.A. Graf von der Schulenburg, J.S. Vrouwenvelder, S.A. Creber, M.C.M. van Loosdrecht and M.L. Johns, Nuclear magnetic resonance microscopy studies of membrane biofouling, J. Membr. Sci., 323 (2008) 37–44.
[3] F.M. Tiller, N.B. Hsyung and D.Z. Cong, Role of porosity in filtration: XII filtration with edimentation, AIChE J., 41 (1995) 1153.
[4] J. Altmann and R. Ripperger, Particle deposition and layer formation at the cross-flow microfiltration, J. Membr. Sci., 124 (1997) 119.
[5] K.L. Tung, S. Wang, W.M. Lu and C.H. Pan, In situ measurement of cake thickness distribution by a photointerrupt sensor, J. Membr. Sci., 190 (2001) 57.
[6] W.M. Lu, K.L. Tung, C.S. Pan and K.J. Hwang, Crossflow microfiltration of monodispersed deformable particle suspension, J. Membr. Sci., 198 (2002) 225.
[7] H. Li, A.G. Fane and S. Vigneswaran, Direct observation of particle deposition on the membrane surface during cross-flow microfiltration, J. Membr. Sci., 149 (1998) 83.
[8] A. Yeo, P. Yang, A.G. Fane, T. White and H.O. Moser, Non-invasive observation of external and internal deposition during membrane filtration by X-ray microimaging (XMI), J. Membr. Sci., 250 (2005) 189–193.
[9] S. Chang, A. Yeo, A.G. Fane, M. Cholewa, P. Yang and H. Moser, Observation of flow characteristics in a hollow fiber lumen using non-invasive X-ray microimaging (XMI), J. Membr. Sci., 304 (2007) 181–189.
[10] K.L. Tung, Y.L. Li, K.J. Hwang and W.M. Lu, Analysis and prediction of fouling layer structure in microfiltration, Desalination, 234 (2008) 99–106.
[11] J.S. Vrouwenvelder, J.A.M. van Paassen, L.P. Wessels, A.F. van Dam and S.M. Bakker, The membrane fouling simulator: A practical tool for fouling prediction and control, J. Membr. Sci., 281 (2006) 316–324.
[12] A.P. Mairal, A.R. Greenberg, W.B. Krantz and L.J. Bond, Real-time measurement of inorganic fouling of RO desalination membranes using ultrasonic time-domain reflectometry, J. Membr. Sci., 159 (1999) 185–196.
[13] A.P. Mairal, A.R. Greenberg and W.B. Krantz, Investigation of membrane fouling and cleaning using ultrasonic time-domain reflectometry, Desalination, 130 (2000) 45–60.
[14] J.X. Li, L.J. Koen, D.K. Hallbauer, L. Lorenzen and R.D. Sanderson, Interpretation of calcium sulfate deposition on reverse osmosis membranes using ultrasonic measurements and a simplified model, Desalination, 186 (2005) 227–241.
[15] T.H. Chong, F.S. Wong and A.G. Fane, Fouling in reverse osmosis: detection by non-invasive techniques, Desalination, 204 (2007) 148–154.
[16] J.X. Li, R.D. Sanderson and G.Y. Chai, A focused ultrasonic sensor for in situ detection of protein fouling on tubular ultrafiltration membranes, Sensor Actuators B, 114 (2006) 182–191.
[17] X.C. Xu, J.X. Li, H.S. Li, Y. Cai, Y.H. Cao, B.Q. He and Y.Z. Zhang, Non-Invasive monitoring of fouling in hollow fiber membrane via UTDR, J. Membr. Sci., 326 (2009) 103–110.
[18] Z.X. Zhang, A.R. Greenberg and W.B. Krantz, Study of membrane fouling and cleaning in spiral wound modules using ultrasonic time-domain reflectometry. In: D. Bhattacharyya and D.A. Butterfield, New Insights into Membrane Science and Technology: Polymeric and Biofunctional Membranes. Elsevier, Amsterdam, 2003.
[19] G.Y. Chai, A.R. Greenberg and W.B. Krantz, Ultrasound, gravimetric, and SEM studies of inorganic fouling in spiral-wound membrane modules, Desalination, 208 (2007) 277–293.
[20] Y.L. Hou, Y.N. Gao, J.X. Li, X.C. Xu and Y. Cai, In-situ monitoring of inorganic and microbial synergistic fouling during nanofiltration by UTDR, Desal. Wat. Treat., 11 (2009) 15–22.
[21] Y.L. Li and K.L. Tung, The effect of curvature of a spacer-filled channel on fluid flow in spiral-wound membrane modules, J. Membr. Sci., 319 (2008) 286–297.
[22] Y.L. Li, K.L. Tung, M.Y. Lu and Sh.H. Huang, Mitigating the curvature effect of the spacer-filled channel in a spiral-wound membrane module, J. Membr. Sci., 329 (2009) 106–118.
[23] Y.L. Li, T.H. Chang, Ch.Y. Wu, Ch.J. Chuang and K.L. Tung, CFD analysis of particle deposition in the spacer-filled membrane module, J. Wat. Supply: Res. Technol.-AQUA, 55(2006) 589–601.
[24] J. Schwinge, P.R. Neal, D.E. Wiley and A.G. Fane, Estimation of foulant deposition across the leaf of a spiral-wound module, Desalination, 146 (2002) 203–208.
[25] T.J. Mason and J.P. Lorimer, Sonochemistry: Theory, Applications and Uses of Ultrasound in Chemistry, Ellis Horwood, Chichester, 1988.
[26] Z.X. Zhang, V.M. Bright and A.R. Greenberg, Use of capacitive microsensors and ultrasonic time-domain reflectometry for in-situ quantification of concentration polarization and membrane fouling in pressure-driven membrane filtration. Sensors Actuators B, 117 (2007) 323–331.